Contrasting glacial meltwater effects on post-bloom phytoplankton on temporal and spatial scales in Kongsfjorden, Spitsbergen

van de Poll, Willem; Kulk, Gemma; Rozema, Patrick; Brussaard, CPD; Visser, Ronald; Buma, Anita

Published in:
Elementa: Science of the Anthropocene

DOI:
10.1525/elementa.307

Publication date:
2018

ELEMENTA
Science of the Anthropocene

van de Poll, WH, et al. 2018. Contrasting glacial meltwater effects on post-bloom phytoplankton on temporal and spatial scales in Kongsfjorden, Spitsbergen. *Elem Sci Anth,* 6: 50. DOI: https://doi.org/10.1525/elementa.307

RESEARCH ARTICLE

Contrasting glacial meltwater effects on post-bloom phytoplankton on temporal and spatial scales in Kongsfjorden, Spitsbergen

Willem H. van de Poll*, Gemma Kulk*, Patrick D. Rozema*, Corina P. D. Brussaard†, Ronald J. W. Visser* and Anita G. J. Buma*,‡

Glacial meltwater discharge in fjords on the west coast of Spitsbergen is increasing due to climate change. The influence of this discharge on phytoplankton nutrient limitation, composition, productivity and photophysiology was investigated in central (M) and inner (G) Kongsfjorden (79°N, 11°40′E). Freshwater influx intensified stratification during June 2015, coinciding with surface nutrient depletion. Surface nutrient concentrations were negatively correlated with stratification strength at station M. Here, nitrate addition assays revealed increasing N limitation of surface phytoplankton during the second half of June, which was followed by a pronounced compositional change within the flagellate-dominated phytoplankton community as dictyochophytes (85% of chl *a*) were replaced with smaller haptophytes (up to 60% of chlorophyll *a*) and prasinophytes (20% of chlorophyll *a*). These changes were less pronounced at station G, where surface phosphate, ammonium and nitrate concentrations were occasionally higher, and correlated with wind direction, suggesting wind-mediated transport of nutrient-enriched waters to this inner location. Therefore, glacial meltwater discharge mediated nutrient enrichment in the inner fjord, and enhanced stratification in inner and central Kongsfjorden. Surface chlorophyll *a* and water column productivity showed 3–4-fold variability, and did not correlate with nutrient limitation, euphotic zone depth, or changed taxonomic composition. However, the maximum carbon fixation rate and photosynthetic efficiency showed weak positive correlations to prasinophyte, cryptophyte, and haptophyte chlorophyll *a*. The present study documented relationships between stratification, N limitation, and changed phytoplankton composition, but surface chlorophyll *a* concentration, phytoplankton photosynthetic characteristics, and water column productivity in Kongsfjorden appeared to be driven by mechanisms other than N limitation.

Keywords: Arctic; phytoplankton; nutrient limitation; pigments; productivity; photophysiology; stratification; meltwater; Kongsfjorden

Introduction

The Arctic is experiencing pronounced changes in climate, which impact the conditions of phytoplankton growth (Arrigo, 2013). Eurasian Arctic regions such as the East Greenland Sea and the Barents Sea have experienced Atlantic inflow with higher heat content (Beszczynska-Möller, 2012; Soltwedel et al., 2015). Increased Atlantic advection and associated relatively high heat content has resulted in decreased wintertime sea ice formation on the west coast of Spitsbergen (Kortsch et al., 2012). This process has also intensified melting of marine-terminating glaciers on the west coast of Spitsbergen and on the east coast of Greenland (Straneo and Heimbach, 2013; Luckman et al., 2015). Atlantic advection in Kongsfjorden occurs in winter and summer, whereas its circulation in the fjord appears to be driven by along-fjord winds (Sundfjord et al., 2017). Atlantic advection can introduce Atlantic phytoplankton and zooplankton populations into fjords like Kongsfjorden (Willis et al., 2008). These changes have transformed the conditions that shape biological activity and diversity on the west coast of Spitsbergen.

As sea ice formation in fjords becomes rare, glacial meltwater of marine-terminating glaciers and meltwater of terrestrial snow and ice become the primary sources of density stratification during spring and summer (MacLachlan et al., 2007; van de Poll et al., 2016; Meire et al., 2017). Surface phytoplankton blooms in Kongsfjorden typically occur after meltwater-induced

* Department of Ocean Ecosystems, Energy and Sustainability Research Institute Groningen, University of Groningen, Nijenborgh 7, 9747 AG Groningen, NL

† NIOZ Royal Netherlands Institute for Sea Research, Department of Marine Microbiology and Biogeochemistry, and Utrecht University, 1790 AB Den Burg, Texel, NL

‡ Arctic Centre, Faculty of Arts, University of Groningen, A-weg 30, 9718 GW Groningen, NL

Corresponding author: Willem H. van de Poll (w.h.van.de.poll@rug.nl)

stratification and subsequently deplete macronutrient stocks as stratification continues throughout the summer (Iversen and Seuthe, 2011). The timing of surface blooms in Kongsfjorden is variable, ranging from April to June (Hegseth and Tverberg, 2013). Stratification during spring and summer can be enhanced by the inflow of warmer Atlantic water. Moreover, freshwater runoff from land can be enhanced due to a rise in air temperature and an intensified hydrological cycle (Luckman et al., 2015; Bintanja and Selten, 2014; Carmack et al., 2016). Despite potential nutrient limitation of surface waters, these coastal fjords maintain relatively high productivity levels during summer, of which the exact mechanisms remain poorly understood. In Kongsfjorden, low N:P ratios suggest nitrogen (N) as the most likely limiting element (Piquet et al., 2014; van de Poll et al., 2016). Moreover, N is suggested to be the primary limiting nutrient in the Arctic at large (Popova et al., 2010). Low nutrient concentrations are a driving factor in phytoplankton succession, typically promoting smaller phytoplankton species, which are more competitive under low nutrient concentrations due to higher surface area to volume ratios (Raven, 1998; Finkel 2001; Lindemann et al., 2016). Changes in phytoplankton size have the potential to directly impact higher trophic levels (Strom and Fredrickson, 2008). However, the extent to which changes in taxonomic composition due to nutrient limitation affect phytoplankton productivity, photophysiology, and biomass in natural phytoplankton communities is uncertain (Palmer et al., 2013).

The present study aimed to assess relationships between salinity stratification, nutrient limitation, and Arctic phytoplankton succession, productivity and photophysiology. Therefore, post-bloom phytoplankton biomass, composition, and productivity were investigated in concert with environmental conditions in inner and central Kongsfjorden, allowing a comparison of variables in the meltwater gradient. Photosynthesis vs irradiance experiments were used to evaluate photosynthetic characteristics and productivity at these stations. Nitrate addition assays were also performed to monitor nitrate limitation in central Kongsfjorden. We expected nitrate limitation at all stations in June due to strong stratification. We hypothesized that phytoplankton productivity would be lower at inner compared to central Kongsfjorden due to increased concentrations of glacial sediment near the marine-terminating glaciers. Colored dissolved organic matter (CDOM), which also influences optical properties of seawater, has been reported to be relatively low in Kongsfjorden (Pavlov et al., 2013).

Methods

Sampling was conducted at two locations in Kongsfjorden, Spitsbergen (79°N, 11°40'E), during June 2015 (**Figure 1**). Station M (central Kongsfjorden, 238 m water depth) and station G (inner Kongsfjorden, 60 m water depth) were visited by boat on eight occasions. Seawater samples were collected at depths of 5.0, 12.5 and 25 m at stations M and G, using a 20-L Niskin bottle, and stored in the dark until processing in the laboratory (within 2 h). Water column profiles were obtained using a CTD (19+, Sea-Bird Electronics) equipped with sensors for PAR [spherical, Licor, Sea-Bird Electronics] and fluorescence [Wetstar]). From the CTD data, the stratification index was calculated as the difference in potential density between depths of 5 and 50 m. Surface mixed layer depth was calculated using the depth of the first buoyancy frequency maximum observed in the upper 50 m. This criterion was found to be ecologically relevant in coastal Antarctic waters (Carvalho et al., 2017). Irradiance attenuation (K_d) was calculated by linear regression of log-transformed PAR data, and the euphotic zone (defined as the depth interval down to 0.1% irradiance) was calculated as: Z_{eu} (m) = –ln (0.001)/K_d. Air temperature and wind direction in Ny Ålesund were collected by the Alfred Wegener Institute Meteorological Surface Measurements.

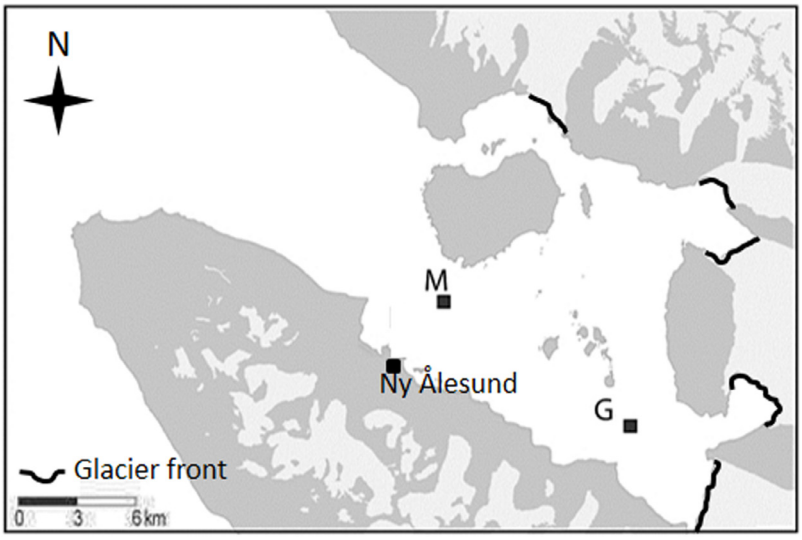

Figure 1: Map of Kongsfjorden, Spitsbergen (79°N, 11°40'E). Indicated are stations M (central Kongsfjorden) and G (inner Kongsfjorden). Black lines indicate the main fronts of marine-terminating glaciers. DOI: https://doi.org/10.1525/elementa.307.f1

Nutrients

Five-mL subsamples (depths of 5, 12.5, 25 m) were filtered (0.2 μm Acrodisc, Pall) for nutrient analysis and stored at –20°C (phosphate, ammonium, nitrate plus nitrite) or 4°C (silicic acid). Nutrient analyses were conducted using a Traacs 800 autoanalyzer (Bran and Luebbe) according to Murphy and Riley (1962), Helder and De Vries (1979), and Grasshoff (1983). Detection limits were 0.01, 0.03, 0.02, and 0.26 μM for phosphate, ammonium, nitrate plus nitrite, and silicic acid, respectively.

Microscopy

Subsamples (5 m, n = 10) for light microscopy (100 mL) from stations M (n = 8) and G (n = 2) were fixed with 1.5 mL Lugol's iodine solution and stored at 4°C in the dark until analysis using an Olympus IMT-2 inverted microscope (Utermöhl technique; Edler and Elbrächter, 2010). The phytoplankton community was semi-quantitatively observed (i.e., not counted) using categories for dictyochophytes, small flagellates, dinoflagellates, and diatoms in settled sample volumes of 5 and 50 ml. Microzooplankton was counted and classified as total ciliates, and small and large dinoflagellates.

Phytoplankton pigment and CHEMTAX analysis

Pigment samples (5.0, 12.5, 25 m) were obtained by mild vacuum filtration (0.2 bar) of 4–10 L seawater on 47 mm GF/F (Whatman) filters. Afterwards, filters were snap-frozen in liquid nitrogen and stored at –80°C until pigment analysis by high performance liquid chromatography (HPLC). For HPLC analysis, filters were freeze-dried for 48 h before extraction in 90% acetone (v/v) for 48 h (4°C, darkness) (van Leeuwe et al., 2006). Pigments were separated by HPLC (Waters 2695) with a Zorbax Eclipse XDB-C8 column (3.5 μm particle size), using the method of Van Heukelem and Thomas (2001). Detection was based on retention time and diode array spectroscopy (Waters 996) at 436 nm. Pigments were quantified manually using standards for all used pigments (DHI lab products). Absolute and relative abundances of phytoplankton groups were assessed by CHEMTAX (version 1.95) (Mackey et al., 1996), which uses factor analysis and steepest descent algorithm to partition pigments between six groups using initial pigment ratios (Table S1). Included groups were based on microscopic observations: prasinophytes, haptophytes, pelagophytes, dictyochophytes, dinoflagellates, and cryptophytes. Diatoms were not observed in light microscopy samples and therefore were not included in CHEMTAX. Results of the haptophyte and pelagophyte sub-groups were pooled (the latter was of minor importance) and were denoted as 'haptophytes'. The pigment data set was split across sampling time and sample depth, resulting in four CHEMTAX bins: samples collected from 5 to 18 June at depths of 5–12.5 m (bin 1, n = 26) and 25 m (bin 2, n = 15). A second pair of bins contained samples collected between 22 and 29 June at depths of 5–12.5 m (bin 3, n = 21) and 25 m (bin 4, n = 6). All pigments were allowed to vary during CHEMTAX analysis (chl *a*: 100%, other pigments: 500%). Initial and final pigment ratios are presented in Table S1.

Depth-integrated chl *a* (upper 50 m) was calculated using reconstructed vertical chl *a* profiles (Figure S1E, F) based on HPLC determined chl *a* and chl *a* fluorescence profiles. The chl *a* fluorescence profiles (5–50 m) were calibrated against HPLC determined chl *a*. Linear relationships of 5 and 12.5 m (used between 5 and 19 m) were different from those obtained at 25 m (used below 19 m). Furthermore, relationships in the upper 12.5 m during 5 to 22 June and 25 to 29 June were different. We assumed equal chl *a* concentrations in the upper 5 m, regardless of chl *a* fluorescence, which was assumed to be influenced by non-photochemical quenching.

Nitrate addition assay (station M only)

Nitrate addition assays were performed using 5-m samples from station M that were collected on eight occasions during the course of June 2015. Subsamples (175 ml) were incubated in acid-washed transparent plastic culture flasks with (nine replicates) and without (nine replicates) nitrate addition (11 μM final concentration) in a cooled incubator (3.5°C) under 20 μmol photons m^{-2} s^{-1} of continuous irradiance (250 W MHNTD lamp, Philips, combined with four layers of neutral density screen). The subsamples were not pre-filtered to exclude grazers. Pigment samples were obtained after 60 h of incubation by mild vacuum filtration (0.2 bar) of 150 ml seawater on 25-mm GF/F (Whatman) filters. Chl *a* concentration was determined using HPLC as described above. Specific growth rates (μ, d^{-1}) were calculated by fitting chl *a* concentrations at the start and end of the incubation period with an exponential function. The differences between the average final chl *a* concentration of nitrate additions and controls were used as a measure for nitrogen limitation (N-limitation index).

Photosynthesis-irradiance (P-E) curves

Photosynthesis-irradiance (P-E) incubations were performed using a modified photosynthetron method (Lewis and Smith, 1983, Rozema et al., 2017). Subsamples (20 ml) collected at 5 m depth at stations M (n = 8) and G (n = 8) were spiked with 10 μl of 0.37 MBq $NaH^{14}CO_3$ and incubated for 3 h at 21 light intensities (15–1500 μmol photons m^{-2} s^{-1}, provided by an Osram power ball HCl-TT 250 W lamp) in 60-ml transparent PET vials in a cryostat-cooled incubator (at *in situ* temperature). Afterwards, samples were filtered onto 0.4 μm pore size polycarbonate filters (25 mm, Milipore), and acidified by HCl fumes under active air filtration (15 min) to remove excess ^{14}C-bicarbonate. Filters were then transferred to 20-ml transparent scintillation vials (PET) and 10 mL of Ultima Gold (Perkin Elmer, the Netherlands) scintillation liquid was added. Vials were vortexed and counted (5 min) after 2 days using a Tri-Carb 2000 CA scintillation counter (Packard). For each P-E incubation three t = 0 samples (^{14}C spiked samples that were directly filtered and acidified) and three total activity samples (100 μl subsamples added to 10 ml of scintillation fluid with 200 μl ethanolamine) were prepared. Carbon incorporation calculations assumed dissolved inorganic carbon (DIC) concentrations of 2100 μmol kg^{-1}. The photosynthetic efficiency (α: mg C mg chl a^{-1} h^{-1}(μmol pho-

tons m^{-2} $s^{-1})^{-1}$), maximum carbon fixation rate (P_{max}: mg C mg chl a^{-1} h^{-1}), and photoinhibition (β: mg C mg chl a^{-1} h^{-1} (μmol photons m^{-2} $s^{-1})^{-1}$) were calculated using the method of Platt et al. (1980). The photoacclimation index was calculated as $E_k = P_{max}/\alpha$ (μmol photons m^{-2} s^{-1}). P-E curves combined with reconstructed vertical chl *a* profiles (Figure S1E, F), light attenuation (K_d) and incident photosynthetically active radiation (PAR) (1 h average, collected by the Baseline Surface Radiation Network, Ny Ålesund, Figure S2A) were used to calculate the daily water column productivity in the euphotic zone (mg C m^{-2} d^{-1}). These calculations assumed identical photophysiological characteristics in the euphotic zone.

Statistics

Linear correlations (Pearson Product Moment) were used to investigate relationships between environmental data. Relationships between environmental and biological data were investigated using non-linear correlations (Spearman Rank Order). Correlations were considered significant at $p < 0.05$. Means are reported with standard deviations. Differences between nitrate addition and controls were tested for significance using a Mann-Whitney U test for each of these assays.

Non-metric multidimensional scaling (NMDS) was applied to the absolute abundances of the phytoplankton groups as estimated by CHEMTAX of the upper 12.5 m (Ramette, 2007). Before analyses, duplicates were averaged and the absolute abundances were transformed using a Box-cox transformation. City-block distances were calculated, as the different groups greatly varied in their scale of change. Clustering was proposed relating to the changes in the community. Both within clusters (between stations) and between clusters (between temporal intervals) were tested for similarity using NP-MANOVAs using the same distance measure (Anderson, 2001). The *p* values were corrected for multiple testing by a Bonferroni correction (Dunn 1961). NMDS and NP-MANOVAs were conducted using Past 2 (Hammer et al., 2001).

Results

Hydrographical conditions at stations M and G

A pronounced difference in potential density between 5 and 50 m established during June at stations M and G (**Figure 2A**). The stratification index increased over time at both stations. Surface salinity (5 m; Figure S1A, B) showed a negative correlation with the stratification index (stations M and G combined, $\rho = -0.97$, $p < 0.0001$). Surface mixed layer depth in June averaged 9 ± 8 and 5 ± 4 m at stations M and G, respectively (results not shown). Sea surface temperature (5 m) increased from 3.2 ± 0.6 (average before June 15) to 5.2 ± 1.0°C at station M during the second half of June (**Figure 2B**; Figure S1C, D), but showed less temporal variability at station G (average: 3.2 ± 0.5°C).

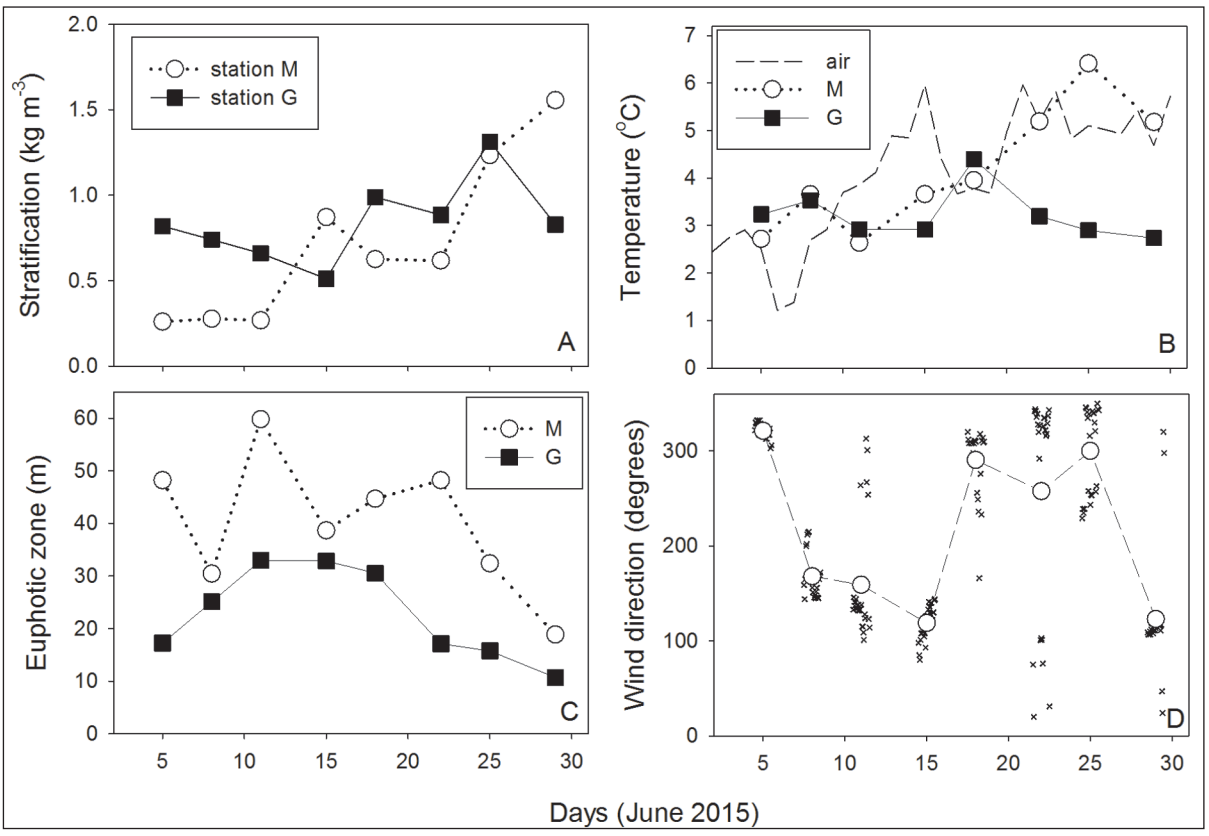

Figure 2: Environmental conditions. Stratification strength (potential density difference between depths of 5 and 50 m) at stations M and G during June 2015 **(A)**. Surface temperature (5 m) at stations M and G, and daily averaged air temperature (Ny Ålesund) **(B)**. Euphotic zone depth (down to 0.1% irradiance) at stations M and G **(C)**. Wind direction (24-h average before sampling) measured in Ny Ålesund **(D)**. The symbol x indicates hourly averaged wind direction during this period. DOI: https://doi.org/10.1525/elementa.307.f2

Mean daily air temperature in Ny Ålesund increased from 2.2 to 5.2°C during the course of June (**Figure 1B**). The euphotic zone (Z_{eu}) was deeper at station M than at station G on every sampling occasion, and shallowed over time at stations M (45 ± 9.9 m to 19 m) and G (33 to 10 m) (**Figure 2C**). Wind direction (24 h average prior to sampling) changed from northwest (321°) to southeast (119°) June 5 to 15, back to northwest (282°) June 18 to 25, and to southeast again at the end of June (**Figure 2D**). Mean wind speed in Ny Ålesund in June was 3.3 ± 2.0 m s^{-1}. Salinity at 75 m at station M showed a negative correlation with wind direction ($\rho = -0.71$, $p = 0.037$).

Nutrient concentrations at stations M and G

Surface (5 m) concentrations of phosphate, ammonium, nitrate plus nitrite, and silicic acid were low in June. Nitrate:phosphate molar ratios at stations M and G were low (mean for upper 25 m: 2.3 ± 1.6 and 4.5 ± 2.4 for M and G, respectively) (data not shown). Surface nutrient concentrations showed different temporal dynamics at stations M and G (**Figure 3**). Surface phosphate and nitrate plus nitrite concentrations correlated negatively with stratification strength at station M but not at station G (**Table 1**). Surface phosphate, ammonium, and nitrate plus nitrite concentrations showed negative correlations with wind direction at station G but not at station M. Surface nutrient concentrations (except silicic acid) at both stations correlated negatively with surface temperature (**Table 1**). Nutrient concentrations (except silicic acid) at 25 m were higher than those at 5 m (**Figure 3**). Phosphate, ammonium, and nitrate plus nitrite concentrations at 25 m increased until June 15 at stations M and G, followed by declines, which were stronger at station M.

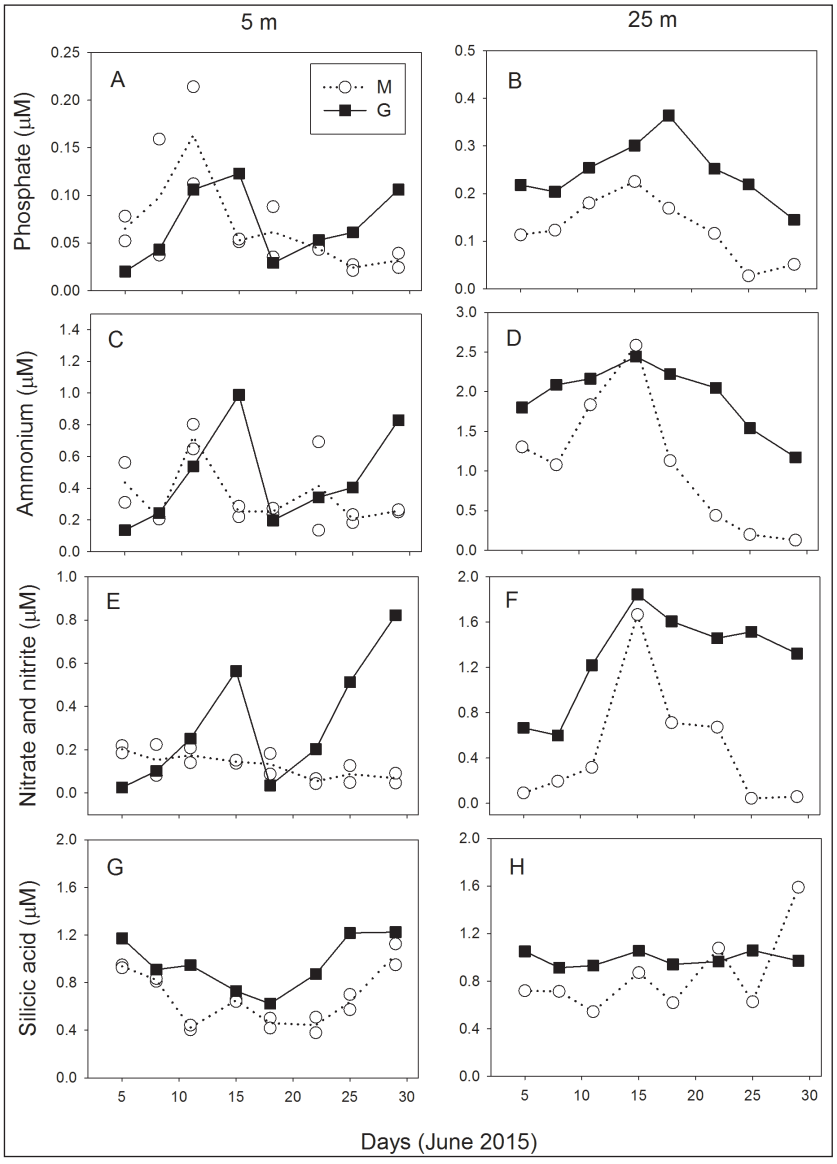

Figure 3: Nutrient concentrations. Phosphate **(A, B)**, ammonium **(C, D)**, nitrate plus nitrite **(E, F)**, and silicic acid **(G, H)** concentrations in surface water (5 m) (A, C, E, G) and at 25-m depth (B, D, F, G) at stations M and G during June 2015. Surface nutrient concentrations at station M are from two individual water samples; other measurements, from a single sample. Note the difference in scale between panels A, C, E, and B, D, F. DOI: https://doi.org/10.1525/elementa.307.f3

Table 1: Pearson correlation coefficients[a] between surface water (5 m) concentrations of phosphate, ammonium, nitrate plus nitrite (NO_3 and NO_2), and silicic acid and stratification strength, surface water (5 m) temperature, and wind direction. DOI: https://doi.org/10.1525/elementa.307.t1

Environmental variable	Station	Surface water (5 m) nutrient concentration			
		Phosphate	Ammonium	$NO_3 + NO_2$	Silicic acid
Stratification	M	–0.67 (0.01)*	–0.41 (0.11)	–0.56 (0.03)*	0.20 (0.46)
	G	–0.51 (0.22)	–0.46 (0.26)	–0.18 (0.66)	0.14 (0.72)
Temperature	M	–0.76 (0.00)*	–0.50 (0.05)	–0.72 (0.00)*	0.024 (0.93)
	G	–0.78 (0.02)*	–0.81 (0.01)*	–0.91 (0.00)*	–0.64 (0.07)
Wind direction[b]	M	–0.15 (0.58)	–0.04 (0.89)	–0.10 (0.72)	–0.03 (0.91)
	G	–0.83 (0.01)*	–0.83 (0.01)*	–0.71 (0.04)*	0.12 (0.75)

[a] Asterisks indicate significant relationships; *p* values are shown in parentheses.
[b] 24-h average prior to sampling.

Table 2: Spearman rank correlation coefficients[a] between surface water (5 m) chlorophyll *a* (chl *a*), depth-integrated chl *a* (0–50 m), and productivity in the euphotic zone (PP_{Zeu}) and stratification strength, surface water (5 m) temperature, wind direction, and N-limitation index. DOI: https://doi.org/10.1525/elementa.307.t2

Environmental variable	Station	Chl *a* (5 m)	Chl *a* (0–50 m)	PP_{Zeu}
Stratification	M	0.24 (0.54)	0.79 (0.00)*	0.17 (0.53)
	G	0.43 (0.30)	0.57 (0.15)	0.11 (0.78)
Temperature	M	–0.19 (0.62)	0.98 (0.00)*	0.29 (0.28)
	G	0.33 (0.39)	0.57 (0.15)	0.89 (0.00)*
Wind direction[b]	M	–0.38 (0.32)	0.00 (0.93)	–0.17 (0.53)
	G	0.71 (0.04)*	0.50 (0.27)	0.25 (0.55)
N-limitation index[c]	M	0.17 (0.66)	0.74 (0.00)*	0.45 (0.08)

[a] Asterisks indicate significant relationships; *p* values are shown in parentheses.
[b] 24-h average prior to sampling.
[c] Available for station M only.

Phytoplankton chlorophyll a and productivity at stations M and G

Surface and depth-integrated chl *a* concentrations at stations M and G showed different temporal dynamics (**Figure 4A, B**; Figure S1E, F). At station M depth-integrated chl *a* (upper 50 m) increased to a maximum of 84 mg m^{-2} on June 25, whereas surface chl *a* peaked on June 15. At station G, surface and depth-integrated chl *a* decreased until June 15, increased towards June 22, and decreased afterwards (**Figure 4B**). Depth-integrated (0–50 m) chl *a* at station M correlated positively to stratification strength and surface temperature (**Table 2**). Surface chl *a* at station G correlated positively to wind direction, which was not observed at station M. Temporal dynamics of daily productivity in the euphotic zone (PP_{Zeu}) were comparable (average for June: 528 ± 246 mg C m^{-2} d^{-1}) for stations M and G (**Figure 4C**). PP_{Zeu} was variable and peaked between June 18 and 22 (average M, G: 901 ± 51 mg C m^{-2} d^{-1}) and declined afterwards to 348 ± 109 mg C m^{-2} d^{-1}. Calculated productivity rates in the upper 5 m of the water column were higher at station G as compared to M, except on June 15 and 29 (Figure S2B, C). PP_{Zeu} showed a positive correlation with surface temperature at station G.

Nitrate limitation assays at station M

The difference in accumulated chl *a* between nitrate addition and control assays increased during the eight assays performed in June (**Figure 5**). The assays showed significant N limitation during the second half of June ($p < 0.001$), with higher chl *a*-based growth rates during nitrate addition from June 15 onwards, as compared to controls without nitrate addition. Prior to June 15, growth rates (mean of controls and N additions) were 0.83 ± 0.2 d^{-1}. From June 15 onwards, growth rates averaged 0.24 ± 0.2 d^{-1} in control assays, and 0.54 ± 0.1 d^{-1} during N addition. The N-limitation index (**Figure 5**) showed positive correlations with stratification strength ($\rho = 0.833$, $p < 0.01$) and depth-integrated chl *a* at station M (**Table 2**).

Phytoplankton composition at stations M and G

Light microscopy revealed dominance of the flagellate *Dictyocha speculum* (Dictyochophyceae, 10–15 μm cell diameter) until June 18 (data not shown). Afterwards, this species declined in abundance, whereas the number of smaller (2–5 μm) unidentified flagellates increased. Furthermore, cryptophytes and small dinoflagellates (<35 μm) were observed more frequently in compari-

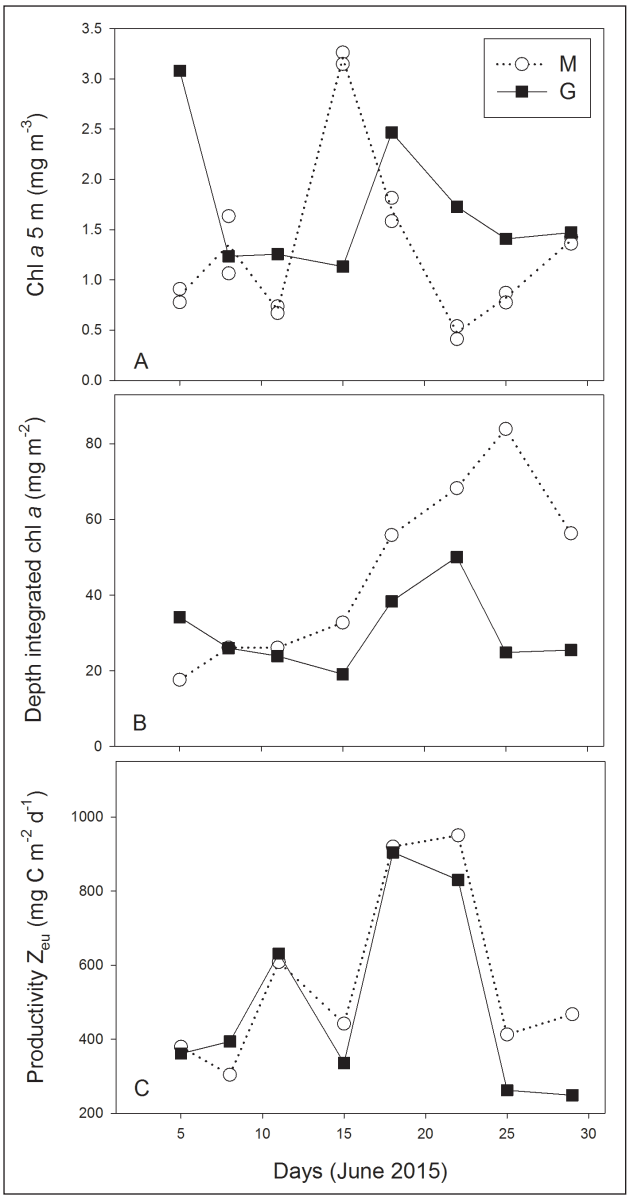

Figure 4: Phytoplankton chlorophyll *a* and productivity. Surface water concentrations of chlorophyll *a* (chl *a* 5 m) **(A)**, depth-integrated chl *a* **(B)**, and productivity in the euphotic zone (Z_{eu}) **(C)** at stations M and G during June 2015. Surface chl *a* concentrations at station M are from two individual water samples; other measurements, from a single sample. Productivity was calculated using carbon fixation characteristics presented in Figure 7. DOI: https://doi.org/10.1525/elementa.307.f4

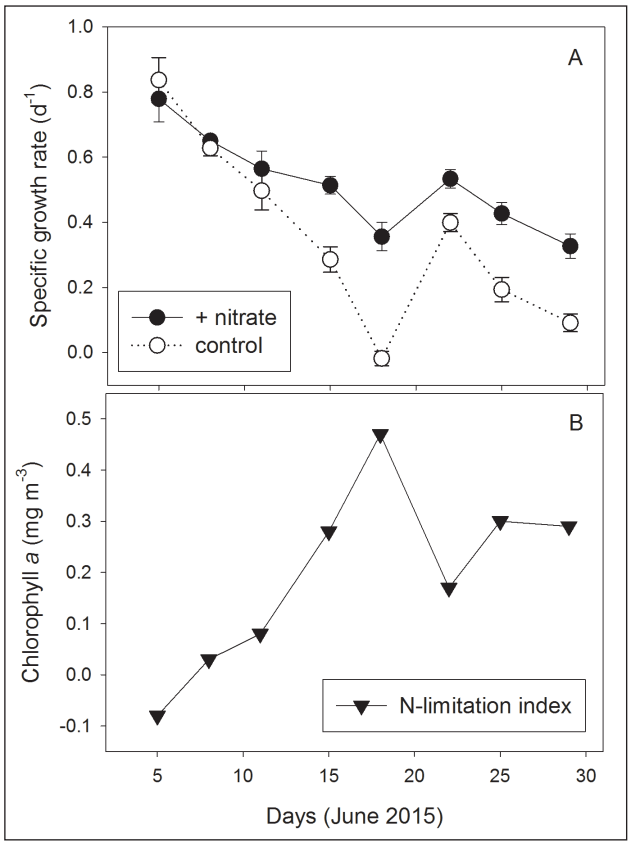

Figure 5: Nitrate addition assays. Chlorophyll *a*-based specific growth rates (d^{-1}) (mean ± standard deviation), with (+ nitrate) and without (control) nitrate addition, as observed during eight consecutive nitrate addition experiments conducted with surface water (5 m) samples collected at central Kongsfjorden **(A)**. Error bars indicate standard deviation of the mean (n = 9 in all cases). N-limitation index: difference in chl *a* concentration between nitrate additions and controls after 60 h of incubation **(B)**. Results are shown on the collection dates of the surface samples (5 m) at station M. DOI: https://doi.org/10.1525/elementa.307.f5

son to early June. Diatoms were absent in all microscopy samples. Microzooplankton changed in concert with photosynthetic phytoplankton at station M. Ciliate concentrations were maximal on June 5 (5080 cells L^{-1}) and declined on June 11 (average 817 ± 449 cells L^{-1}). *Gyrodinium spirale* (Dinophyceae) averaged 1705 ± 835 cells L^{-1} until June 15 and increased to 8660 cells L^{-1} on June 29, whereas large unidentified dinoflagellate concentrations averaged 20 ± 21 cells L^{-1}. CHEMTAX analysis showed a dominance of dictyochophyte chl *a* until June 18 (average 86% of chl *a*) and a decline of this taxonomic group afterwards (**Figure 6A**). The decline in surface dictyochophytes was more pronounced at station M as compared to G. By the end of June, the relative abundance of dictyochophytes reduced to less than 1% of chl *a* at station M. In contrast, surface prasinophytes, cryptophytes, and haptophytes increased in relative and absolute abundance after June 18 at stations M and G (**Figure 6C, E, G**). Absolute prasinophyte, cryptophyte, and haptophyte chl *a* showed positive correlations to stratification strength and the N-limitation index (station M only) (**Table 3**). Relative cryptophyte abundance at 25 m decreased at stations M and G over time (**Figure 6F**). Peridinin-containing dinoflagellates showed a low relative abundance, contributing between 0.5 and 3% to chl *a* (not shown).

Clustering (NMDS) showed significant grouping of stations M and G from June 5 to 11, where samples of M and G were not different (Figure S3). A second cluster was observed for M and G from June 22 to 29 that was significantly different from the first cluster (pseudo-F = 23.75, $p < 0.001$). Within the second cluster, samples of M and G were significantly different (Bonferroni corrected Manhattan distance, F = 3.856, $p < 0.05$).

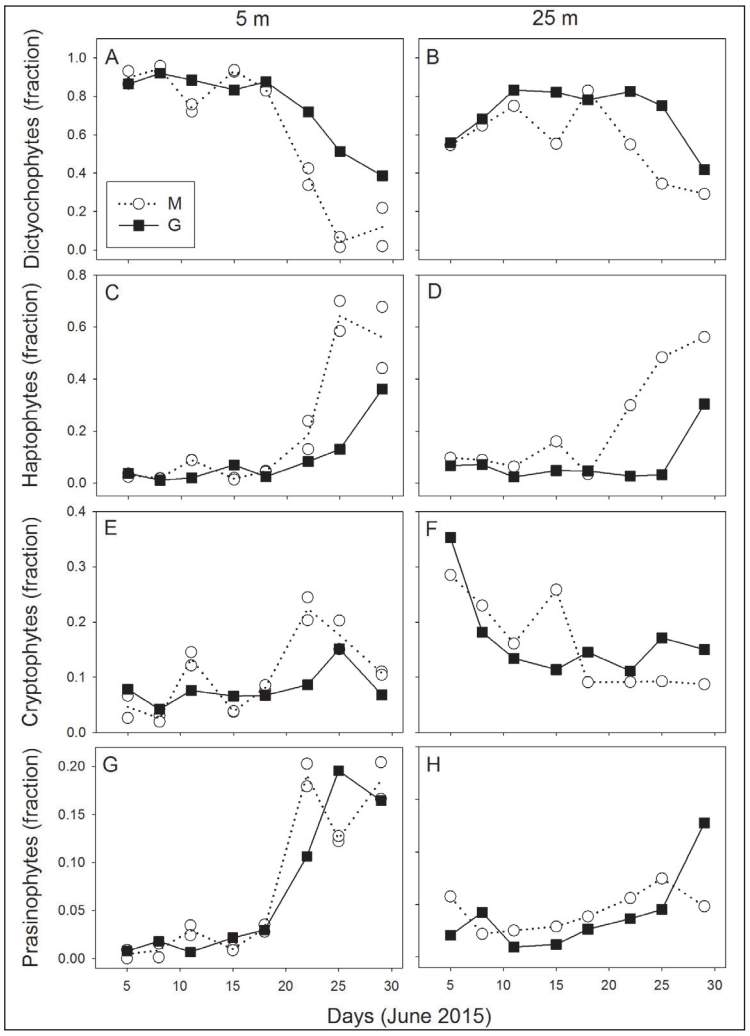

Figure 6: Relative abundance of phytoplankton taxonomic groups. Relative abundance (fraction of chlorophyll *a*) of dictyochophytes **(A, B)**, haptophytes **(C, D)**, cryptophytes **(E, F)**, and prasinophytes **(G, H)** at stations M and G, shown for samples collected at depths of 5 m (A, C, E, G) and 25 m (B, D, F, H). Surface relative abundance at station M are from two individual water samples; other measurements, from a single sample. DOI: https://doi.org/10.1525/elementa.307.f6

Table 3: Spearman rank correlation coefficients[a] between surface water (5 m) prasinophyte, cryptophyte, dictyochophyte, and haptophyte chlorophyll *a* (chl *a*) and surface water (5 m) temperature, stratification strength, euphotic zone depth and N-limitation index. DOI: https://doi.org/10.1525/elementa.307.t3

Environmental variable	Chl *a* (absolute amount) by phytoplankton taxon			
	Prasinophyte	Cryptophyte	Dichtyochophyte	Haptophyte
Stratification	0.81 (0.00)*	0.79 (0.00)*	–0.13 (0.55)	0.72 (0.00)*
Temperature	0.52 (0.01)*	0.42 (0.04)*	–0. 21 (0.32)	0.41 (0.05)*
Euphotic zone	–0.53 (0.01)*	–0.45 (0.03)*	–0.09 (0.67)	–0.51 (0.01)*
N-limitation index	0.79 (0.00)*	0.83 (0.00)*	–0.16 (0.55)	0.81 (0.00)*

[a] Correlations were with stations M and G combined except for the N-limitation index, which was determined at station M only. Asterisks indicate significant relationships; *p* values are shown in parentheses.

Carbon fixation characteristics and photophysiology at stations M and G

Maximum carbon fixation rate (P_{max}) increased at station M after June 15 from 1.5 ± 0.5 to 2.7 ± 0.4 μg C chl a^{-1} h^{-1}, whereas this increasing trend was not observed at station G (mean of 2.1 ± 0.5 μg C chl a^{-1} h^{-1}) (**Figure 7A**). The photosynthetic efficiency (α) was higher at station G compared to station M (except on June 29) (**Figure 7B**). Photosynthetic efficiency increased, whereas the photoacclimation index (E_k) decreased during the course of June (**Figure 7C**). This decrease was most pronounced at station M, where E_k declined from 125 ± 20 (until June 15) to 93 ± 5 μmol photons m^{-2} s^{-1}. At station G the average E_k was 81 ± 22 μmol photons m^{-2} s^{-1}. The E_k at station M correlated nega-

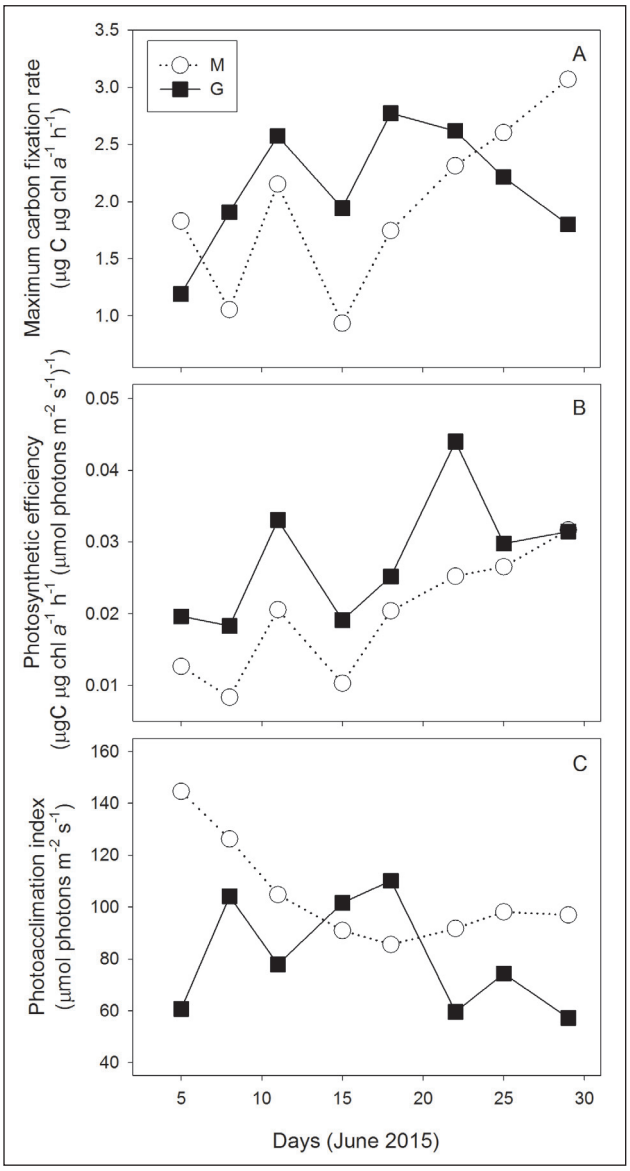

Figure 7: Characteristics of phytoplankton carbon fixation. Maximum carbon fixation rate **(A)**, photosynthetic efficiency **(B)**, and photoacclimation index **(C)**, in surface water samples (5 m) at stations M and G. DOI: https://doi.org/10.1525/elementa.307.f7

tively to the N-limitation index, and positively to euphotic zone depth. The α and P_{max} showed weak positive correlations with relative prasinophyte, cryptophyte, and haptophyte abundance, and negative correlations with relative dictyochophyte abundance (**Table 4**). In addition, α correlated positively to the stratification index (**Table 4**). The E_k at station M correlated negatively to the N-limitation index and positively to euphotic zone depth (**Table 4**). Photoinhibition (β) averaged 0.0014 ± 0.0016 mg C mg chl a^{-1} h^{-1} (µmol photons m^{-2} $s^{-1})^{-1}$ and did not show a temporal trend.

Discussion

The surface phytoplankton community experienced nutrient depletion in June 2015, with chl *a* concentrations that were typical for the post-bloom period in June (Hegseth and Tverberg, 2013; van de Poll et al., 2016). Furthermore, the higher ammonium than nitrate concentrations that we observed in June suggest that productivity in Kongsfjorden was regulated by remineralization of nutrients. These nutrient conditions coincided with a phytoplankton community that was dominated by flagellates and their grazers, which were previously shown to be an important component of post-bloom phytoplankton in Kongsfjorden (Iversen and Seuthe, 2011; Seuthe et al., 2011). In the present study, stratification mediated by freshwater was strong and further increased during June. The average potential density difference between 5 and 50 m was 45-fold higher in June 2015 compared to observations in April 2014 (van de Poll et al., 2016). Stratification strength in June was comparable to stratification in the oligotrophic North East Atlantic but lower than maximum stratification strength in the Canada Basin (van de Poll et al., 2013; Tremblay et al., 2015).

The nitrate addition assays showed that surface phytoplankton growth in central Kongsfjorden was limited by nitrogen from June 15 onwards, coinciding with increasing stratification. N limitation was also suggested by the overall low inorganic N:P ratios, although a temporal trend in N:P was not observed. Decreasing growth rates of controls and nitrate addition treatments, combined with low phosphate and silicic acid concentrations, could signal

Table 4: Spearman rank correlation coefficients[a] between maximum carbon fixation rate (P_{max}), photosynthetic efficiency (α), and photoacclimation index (E_k) at 5 m depth and stratification strength, surface temperature, euphotic zone depth, N-limitation index, and relative abundance of prasinophyte, cryptophyte, dictyochophyte, and haptophyte chl *a*. DOI: https://doi.org/10.1525/elementa.307.t4

Variable	P_{max}	α	E_k
Stratification	0.51 (0.05)	0.58 (0.02)*	–0.44 (0.10)
Temperature	0.26 (0.33)	0.03 (0.90)	0.08 (0.80)
Euphotic zone	–1.3 (0.63)	–0.42 (0.12)	0.56 (0.03)*
N-limitation index	0.29 (0.46)	0.52 (0.16)	–0.81 (0.01)*
Prasinophyte chl *a* (fraction)	0.54 (0.03)*	0.55 (0.03)*	–0.19 (0.46)
Cryptophyte chl *a* (fraction)	0.56 (0.03)*	0.67 (0.005)*	–0.37 (0.16)
Dichtyochophyte chl *a* (fraction)	–0.54 (0.03)*	–0.65 (0.01)*	0.32 (0.22)
Haptophyte chl *a* (fraction)	0.48 (0.06)*	0.62 (0.01)*	–0.34 (0.19)

[a] Correlations were with stations M and G combined except for the N-limitation index, which was determined at station M only. Asterisks indicate significant relationships; *p* values are shown in parentheses.

the possibility of phosphate and silicic acid co-limitation during the second half of June.

The onset of N limitation as detected by the assays was followed by a pronounced change in phytoplankton taxonomic composition from a dictyochophyte-dominated phytoplankton community to one dominated by haptophytes and prasinophytes, with subsequent changes in cell size (dictyochophytes: 10–15 μm; haptophytes: 5 μm; prasinophytes: 2 μm). Smaller phytoplankton species are believed to be more competitive during low nutrient concentrations due to a high surface area to volume ratio (Raven, 1998; Li et al., 2009; Finkel 2001; Lindemann et al., 2016). The change in phytoplankton composition showed considerable delay compared to the onset of N limitation. This delay may be related to different conditions during the assays in comparison to *in situ* conditions, such as grazing pressure from large zooplankton. However, the photoacclimation index and daily experienced irradiance showed that irradiance conditions during the assays were 4–5-fold lower than those experienced at 5-m depth in central Kongsfjorden. Given the relatively low light conditions used in the assays, the observed response to nitrate enrichment should be considered conservative, and thus to underscore the severity of nitrate limitation in situ in the surface waters.

The pronounced change in phytoplankton taxonomic composition was not clearly reflected in surface chl *a* concentrations, which were variable (up to 4-fold differences) and showed no relationship with stratification strength or N limitation at station M. Thee findings are in line with observations in the Canada Basin, where mean surface chl *a* did not change in relation to decreasing nutrient concentrations, while changes in the phytoplankton community were evident on a temporal scale (Li et al., 2009). In the present study, stratification coincided with increased depth-integrated chl *a* at station M and reduced nutrient concentrations at 25 m. Chl *a* accumulation at depth at station M was around the base of the euphotic zone and therefore exerted a limited effect on productivity. In contrast, reduced light penetration due to glacial sediment presumably prevented the build-up of depth-integrated chl *a* at station G, thereby maintaining higher nutrient concentrations close to the surface. Glacial melting at inner Kongsfjorden coincides with sediment influx, thereby increasing light attenuation (Piquet et al., 2014; van de Poll et al., 2016; this study). This effect is widely believed to limit productivity in inner Kongsfjorden (Wiencke and Hop, 2016). However, our productivity estimates did not show consistent differences in water column productivity between inner and central Kongsfjorden, in spite of a shallower euphotic zone at station G. Observations in April and May showed a stronger contrast in irradiance attenuation and hydrographical conditions between central and inner Kongsfjorden (van de Poll et al., 2016), as compared to June. Our observations were prior to the peak sediment and glacial meltwater discharge in Kongsfjorden (July and August).

Surface nutrient concentrations at station G were occasionally higher than those at station M, and showed dynamics that correlated with wind direction. Increased summertime nutrient concentrations at inner compared to central Kongsfjorden were previously observed in July 2014, but not in 2013 (Fransson et al., 2016). This phenomenon was suggested to be caused by upwelling of fresh glacial meltwater (Lydersen et al., 2014). In the present study, the nutrient-enriched water may have been transported to our sampling site at inner Kongsfjorden due to out-of-fjord winds from the southeast. Moreover, a chl *a* peak was observed three days after the nutrient spike, suggesting that nutrient-enriched surface water triggered elevated biological activity at inner Kongsfjorden. Furthermore, changes in phytoplankton composition were less pronounced at station G as compared to M, suggesting a reduced effect of N limitation at the former site. Our data do not show relationships that point to wind-related nutrient enrichment effects beyond inner Kongsfjorden. Nevertheless, surface chl *a* at station M peaked on the day of enrichment at station G. The negative correlation of salinity at depth at station M and wind direction suggests that the same process caused advection of deep saline water, coinciding with increased nutrient concentrations at 25 m. Possibly, episodic wind-mediated transport of nutrient-enriched water masses could explain the patchiness of chl *a* concentrations and productivity during the stratified summer period in Kongsfjorden.

Similar to surface chl *a*, water column productivity showed 4-fold differences on temporal scales, but no significant trends in relation to N limitation, stratification, or taxonomic changes. Carbon fixation characteristics showed variability that was weakly correlated to phytoplankton composition. The overall effect of these changes on water column productivity appeared to be limited. The differences in chl *a*-specific carbon fixation characteristics may arise from cell size and changes in cellular chl *a* related to chl *a* self-shading. Palmer et al. (2013) reported no change in chl *a*-specific maximum photosynthetic rates when comparing the characteristics of nutrient-limited surface and irradiance-limited sub-surface chlorophyll maxima of coastal and open ocean phytoplankton in the Chukchi and Beaufort Sea. In contrast, higher chl *a*-specific maximum photosynthetic rates were associated with diatoms as compared to flagellate-dominated communities in the Labrador Sea (Fragoso et al., 2016). We observed a trend of increasing photosynthetic efficiency (and decreasing photoacclimation index) in response to decreasing irradiance in Kongsfjorden. This trend may represent the classical photoacclimation response of increased light harvesting efficiency under reduced irradiance or, alternatively, may be due to taxon-specific changes (Palmer et al., 2011, 2013). At present, the comparative roles of photoacclimation and the taxonomic components in determining carbon fixation characteristics could not be elucidated. Sources of error in our productivity estimates include uncertainties related to the vertical chl *a* distribution and that our sampling scheme did not account for photoacclimation, which can influence carbon fixation characteristics in stratified systems.

In conclusion, nitrate limitation assays revealed increasing N limitation in the surface waters of central Kongsfjorden in June, coinciding with increasing stratification strength. N limitation was followed by a change in taxonomic composition and size structure of the phytoplankton community, suggesting that N limitation was

a driver of taxonomic succession in Kongsfjorden post-bloom phytoplankton. However, the complete change in phytoplankton composition in the current study was not accompanied by trends in surface water chl *a* or water column productivity. Furthermore, we observed differences in surface nutrient concentrations between central and inner Kongsfjorden, presumably due to upwelling in the proximity of the glacier front and subsequent episodic wind-induced transport out of the fjord. Therefore, nutrient limitation appeared to be less pronounced in inner as compared to central Kongsfjorden. Our investigation suggests that glacial meltwater has contrasting effects on phytoplankton on temporal and spatial scales by influencing both stratification and upwelling processes. Summertime stratification by glacial meltwater influx, melting sea ice, and/or terrestrial runoff from snow and ice melt is an annually occurring process in Kongsfjorden (Hop et al., 2002). Glacial calving has previously been shown to be governed by seawater temperature in Kongsfjorden (Luckman et al., 2015), so that years with strong Atlantic advection can be expected to have a stronger summertime glacial meltwater component governing stratification (Fransson et al., 2016). Consequently, years with stronger Atlantic advection and stronger summertime stratification may experience a stronger shift in post-bloom phytoplankton community and size structure in central Kongsfjorden. However, warming of the fjord may also increase nutrient upwelling near the glaciers due to elevated glacial meltwater discharge. Whether this scenario also causes a stronger contrast between inner and central Kongsfjorden remains to be elucidated. The observed environmental changes in Kongsfjorden of the past decades have the potential to influence nutrient limitation, phytoplankton composition, and thereby higher trophic levels, making these processes and their relation to stratification in Kongsfjorden deserving of further investigation.

Data Accessibility Statement

https://doi.pangaea.de/10.1594/PANGAEA.878242.

Supplemental files

The supplemental files for this article can be found as follows:

- **Table S1.** Initial (A) and final (B) pigment ratios for CHEMTAX taxonomic groups relative to chlorophyll *a*. DOI: https://doi.org/10.1525/elementa.307.s1
- **Figure S1.** Salinity, temperature and reconstructed chl *a* profiles. DOI: https://doi.org/10.1525/elementa.307.s1
- **Figure S2.** Irradiance and productivity profiles. DOI: https://doi.org/10.1525/elementa.307.s1
- **Figure S3.** NMDS of phytoplankton composition. DOI: https://doi.org/10.1525/elementa.307.s1

Acknowledgements

We thank the technical and scientific staff of the Alfred Wegener Institute for facilitating our research at the AWIPEV research base, and for providing the meteorological data. Furthermore, we thank the Kingsbay Marine lab staff for their assistance. Special thanks to Loes A. H. Venekamp for the light microscopy analysis.

Funding informations

This work is a contribution to NWO project 866.12.408 (Buma) and 866.12.404 (Brussaard).

Competing interests

The authors have no competing interests to declare.

Author contributions

- WHvdP: contributed to design, data acquisition, analysis and interpretation.
- GK: contributed to data acquisition, analysis and interpretation.
- PDR: contributed to analysis and interpretation.
- CPDB: contributed to analysis and interpretation.
- RJWV: contributed to analysis and interpretation.
- AGJB: contributed to analysis and interpretation.

References

Anderson, MJ. 2001. A new method for non-parametric multivariate analysis of variance. *Austral Ecology* **26**: 32–46.

Arrigo, KR. 2013. The changing Arctic Ocean. *Elem Sci Anth* **1**: 10. DOI: https://doi.org/10.12952/journal.elementa.000010

Beszczynska-Möller, A, Fahrbach, E, Schauer, U and **Hansen, E.** 2012. Variability in Atlantic water temperature and transport at the entrance to the Arctic Ocean, 1997–2010. *ICES J Marine Sci* **69**(5): 852–863. DOI: https://doi.org/10.1093/icesjms/fss056

Bintanja, R and **Selten, FM.** 2014. Future increases in Arctic precipitation linked to local evaporation and sea-ice retreat. *Nature* **509**: 479–482. DOI: https://doi.org/10.1038/nature13259

Carmack, EC, Yamamoto-Kawai, M, Haine, TWN, Bacon, S, Bluhm, BA, Lique, C, Melling, H, Polyakov, IV, Straneo, F, Timmermans, M-L and **Williams, WJ.** 2016. Freshwater and its role in the Arctic Marine System: Sources, disposition, storage, export, and physical and biogeochemical consequences in the Arctic and global oceans. *J Geophys Res Biogeosci* **121**: 675–717. DOI: https://doi.org/10.1002/2015JG003140

Carvalho, F, Kohut, J, Oliver, MJ and **Schofield, O.** 2017. Defining the ecologically relevant mixed layer depth for Antarctica's Coastal Seas. *Geophys Res Let* **44**(1): 338–345. DOI: https://doi.org/10.1002/2016GL071205

Dunn, OJ. 1961. Multiple Comparisons Among Means. *Journal of the American Statistical Association* **56**: 52–64. DOI: https://doi.org/10.1080/01621459.1961.10482090

Edler, L and **Elbrächter, M.** 2010. The Utermöhl method for quantitiative phytoplankton analysis. In: Karlson, B, Cusack, C and Bresnan, E (eds.), *Microscopic and molecular methods for quantitiative phytoplankton analysis*. Paris: Intergovernmental Oceanographic Commission of © UNESCO.

Finkel, ZV. 2001. Light absorption and size scaling of light limited metabolism in marine diatoms. *Limnol Oceanogr* **46**: 86–94. DOI: https://doi.org/10.4319/lo.2001.46.1.0086

Fragoso, GM, Poulton, AJ, Yashayaev, IM, Head, EJH and **Purdie, DA.** 2016. Spring phytoplankton communities of the Labrador Sea (2005–2014): pigment signatures, photophysiology and elemental ratios. *Biogeosciences* **14**: 1235–1259. DOI: https://doi.org/10.5194/bg-2016-295

Fransson, A, Chierici, M, Hop, H, Findlay, HS, Kristiansen, S and **Wold, A.** 2016. Late winter-to-summer change in ocean acidification state in Kongsfjorden, with implications for calcifying organisms. *Polar Biol* **39**: 1841–1857. DOI: https://doi.org/10.1007/s00300-016-1955-5

Grasshoff, K. 1983. Determination of nitrate. In: Grasshoff, K, Erhardt, M and Kremeling, K (eds.), *Methods of seawater analysis*, 143–150. Verlag Chemie: Weinheim, Germany.

Hammer, Ø, Harper, DAT and **Ryan, PD.** 2001. PAST: Paleontological statistics software package for education and data analysis. *Palaeontologia Electronica* **4**(1): 9.

Hegseth, EN and **Tverberg, V.** 2013. Effect of Atlantic water inflow on timing of the phytoplankton spring bloom in a high Arctic fjord (Kongsfjorden, Svalbard). *J Marine Syst* **113–114**: 94–105. DOI: https://doi.org/10.1016/j.jmarsys.2013.01.003

Helder, W and **De Vries, RTP.** 1979. An automatic phenol-hypochlorite method for the determination of ammonia in sea- and brackish waters. *Neth J Sea Res* **13**: 154–160. DOI: https://doi.org/10.1016/0077-7579(79)90038-3

Hop, H, Pearson, T, Hegseth, EN, Kovacs, KM, Wiencke, C and **Kwasniewski, S.** 2002. The marine ecosystem of Kongsfjorden in Svalbard. *Polar Res* **21**: 167–208. DOI: https://doi.org/10.1111/j.1751-8369.2002.tb00073.x

Iversen, KR and **Seuthe, L.** 2011. Seasonal microbial processes in a high-latitude fjord (Kongsfjorden, Svalbard): I. Heterotrophic bacteria, picoplankton and nanoflagellates. *Polar Biol* **34**: 731–749. DOI: https://doi.org/10.1007/s00300-010-0929-2

Kortsch, S, Primicerio, R, Beuchel, F, Renaud, PE, Rodrigues, J, Lønne, OJ and **Gulliksen, B.** 2012. Climate-driven regime shifts in Arctic marine benthos. *Proc Natl Acad Sci USA* **109**(35): 14052–14057. DOI: https://doi.org/10.1073/pnas.1207509109

Lewis, M and **Smith, J.** 1983. A small volume, short-incubation-time method for measurement of photosynthesis as a function of incident irradiance. *Mar Ecol Prog Ser* **13**: 99–102. DOI: https://doi.org/10.3354/meps013099

Li, WKW, McLaughlin, FA, Lovejoy, C and **Carmack, EC.** 2009. Smallest algae thrive as the Arctic Ocean freshens. *Science* **326**: 539–539. DOI: https://doi.org/10.1126/science.1179798

Lindemann, C, Fiksen, Ø, Andersen, KH and **Aksnes, DL.** 2016. Scaling laws in phytoplankton nutrient uptake affinity. *Front Mar Sci.* DOI: https://doi.org/10.3389/fmars.2016.00026

Luckman, A, Benn, DI, Cottier, F, Bevan, S, Nilsen, F and **Inall, M.** 2015. Calving rates at tidewater glaciers vary strongly with ocean temperature. *Nat Commun* **6**: 8566. DOI: https://doi.org/10.1038/ncomms9566

Lydersen, C, Assmy, P, Falk-Petersen, S, Kohler, J, Kovacs, KM, Reigstad, M, Steen, H, Strøm, H, Sundfjord, A, Varpe, O, Walczowski, W, Weslawski, JM and **Zajaczkowski, M.** 2014. The importance of tidewater glaciers for marine mammals and seabirds in Svalbard, Norway. *J Mar Sys* **129**: 452–471. DOI: https://doi.org/10.1016/j.jmarsys.2013.09.006

Meire, L, Mortensen, J, Meire, P, Juul-Pedersen, T, Sejr, MK, Rysgaard, S, Nygaard, R, Huybrechts, P and **Meysman, FJR.** 2017. Marine-terminating glaciers sustain high productivity in Greenland fjords. *Global Change Biol* **23**(12): 5344–5357. DOI: https://doi.org/10.1111/gcb.13801

Mackey, MD, Higgins, HW, Mackey, DJ and **Wright, SW.** 1996. CHEMTAX – a program for estimating class abundances from chemical markers: application to HPLC measurements of phytoplankton. *Mar Ecol Prog Ser* **144**: 265–283. DOI: https://doi.org/10.3354/meps144265

MacLachlan, SE, Cottier, FR, Austin, WEN and **Howe, JA.** 2007. The salinity: $d^{18}O$ water relationship in Kongsfjorden, western Spitsbergen. *Polar Res* **26**: 160–167. DOI: https://doi.org/10.1111/j.1751-8369.2007.00016.x

Murphy, J and **Riley, JP.** 1962. A modified single solution method for the determination of phosphate in natural waters. *Analytica Chimica Acta* **27**: 31–36. DOI: https://doi.org/10.1016/S0003-2670(00)88444-5

Palmer, MA, Arrigo, KR, Mundy, CJ, Ehn, JK, Gosselin, M, Barber, DG, Martin, J, Alou, E, Roy, S and **Tremblay, JÉ.** 2011. Spatial and temporal variation of photosynthetic parameters in natural phytoplankton assemblages in the Beaufort Sea, Canadian Arctic. *Polar Biol* **34**: 1915–1928. DOI: https://doi.org/10.1007/s00300-011-1050-x

Palmer, MA, van Dijken, GL, Mitchell, BG, Seegers, BJ, Lowry, KE, Mills, MM and **Arrigo, KR.** 2013. Light and nutrient control of photosynthesis in natural phytoplankton populations from the Chukchi and Beaufort seas, Arctic Ocean. *Limnol Oceanogr* **58**(6): 2185–2205. DOI: https://doi.org/10.4319/lo.2013.58.6.2185

Pavlov, AK, Silyakova, A, Granskog, MA, Bellerby, RGJ, Engel, A, Schulz, KG and **Brussaard, CPD.** 2013. Marine CDOM accumulation during a coastal Arctic mesocosm experiment: No response to elevated pCO_2 levels. *J Geophys Res: Biogeoscience* **119**(6): 1216–1230. DOI: https://doi.org/10.1002/2013JG002587

Piquet, AMT, van de Poll, WH, Visser, RJW, Wiencke, C, Bolhuis, H and **Buma, AGJ.** 2014. Springtime phytoplankton dynamics in the Arctic Krossfjorden and Kongsfjorden (Spitsbergen) as a function of glacier proximity. *Biogeosciences* **11**: 2263–2279. DOI: https://doi.org/10.5194/bg-11-2263-2014

Platt, T, Gallegos, CL and **Harrison, WG.** 1980. Photoinibition of photosynthesis in atural assemblages of marine phytoplankton. *J Mar Res* **38**: 687–701.

Popova, EE, Yool, A, Coward, AC, Aksenov, YK, Alderson, SG, de Cuevas, BA and **Anderson, TR.** 2010. Control of primary production in the Arctic by nutrients and light: insights from a high resolution ocean general circulation model. *Biogeosciences* **7**: 3569–3591. DOI: https://doi.org/10.5194/bg-7-3569-2010

Ramette, A. 2007. Multivariate analyses in microbial ecology. *FEMS Microbiol Ecol* **62**: 142–160. DOI: https://doi.org/10.1111/j.1574-6941.2007.00375.x

Raven, JA. 1998. The twelfth Tansley Lecture. Small is beautiful: the picophytoplankton. *Funct Ecol* **2**: 503–513. DOI: https://doi.org/10.1046/j.1365-2435.1998.00233.x

Rozema, PD, Kulk, G, Veldhuis, MP, Buma, AGJ, Meredith, MP and **van de Poll, WH.** 2017. Assessing drivers of coastal phytoplankton productivity in northern Marguerite Bay, Antarctica. *Front Mar Sci* **4**. DOI: https://doi.org/10.3389/fmars.2017.00184

Seuthe, L, Iversen, KR and **Narcy, F.** 2011. Microbial processes in a high-latitude fjord (Kongsfjorden, Svalbard): II. Ciliates and dinoflagellates. *Polar Biol* **34**: 751–76. DOI: https://doi.org/10.1007/s00300-010-0930-9

Soltwedel, T, Bauerfeind, E, Bergmann, M, Bracher, A, Budaeva, N, Busch, K, Cherkasheva, A, Fahl, K, Grzelak, K, Hasemann, C, Jacob, M, Kraft, A, Lalande, C, Metfies, K, Nöthig, EM, Meyer, K, Quéric, N-V, Schewe, I, Włodarska-Kowalczuk, M and **Klages, M.** 2015. Natural variability or anthropogenically-induced variation? Insights from 15 years of multidisciplinary observations at the arctic marine LTER site HAUSGARTEN. *Ecol Indic* **65**: 89–102. DOI: https://doi.org/10.1016/j.ecolind.2015.10.001

Straneo, F and **Heimbach, P.** 2013. North Atlantic warming and the retreat of Greenland's outlet glaciers. *Nature* **504**: 36–43. DOI: https://doi.org/10.1038/nature12854

Sundfjord, A, Albretsen, J, Kasajima, Y, Skogseth, R, Kohler, J, Nuth, C, Skarðhamar, J, Cottier, F, Nilsen, F, Asplin, L, Gerland, S and **Torsvik, T.** 2017. Effects of glacier runoff and wind on surface layer dynamics and Atlantic Water exchange in Kongsfjorden, Svalbard; a model study. *Estuar Coast Shelf S* **187**: 260–272. DOI: https://doi.org/10.1016/j.ecss.2017.01.015

Tremblay, JÉ, Anderson, LG, Matrai, P, Coupel, P, Bélanger, S, Michel, C and **Reigstad, M.** 2015. Global and regional drivers of nutrient supply, primary production and CO_2 drawdown in the changing Arctic Ocean. *Prog Oceanogr* **139**: 171–196. DOI: https://doi.org/10.1016/j.pocean.2015.08.009

van de Poll, WH, Kulk, G, Timmermans, KR, Brussaard, CPD, van der Woerd, HJ, Kehoe, MJ, Mojica, KDA, Visser, RJW, Rozema, PD and **Buma, AGJ.** 2013. Phytoplankton chlorophyll *a* biomass, composition and productivity along a temperature and stratification gradient in the North East Atlantic Ocean. *Biogeosciences* **10**: 4227–4240. DOI: https://doi.org/10.5194/bg-10-4227-2013

van de Poll, WH, Maat, DS, Fischer, P, Rozema, PD, Daly, OB, Koppelle, S, Visser, RJW and **Buma, AGJ.** 2016. Atlantic advection driven changes in glacial meltwater: Effects on phytoplankton chlorophyll *a* and taxonomic composition in Kongsfjorden, Spitsbergen. *Front Mar Sci*. DOI: https://doi.org/10.3389/fmars

Van Heukelem, L and **Thomas, CS.** 2001. Computer-assisted high-performance liquid chromatography method development with applications to the isolation and analysis of phytoplankton pigments. *J Chromatogr A* **910**: 31–49. DOI: https://doi.org/10.1016/S0378-4347(00)00603-4

van Leeuwe, MA, Villerius, LA, Roggeveld, J, Visser, RJW and **Stefels, J.** 2006. An optimized method for automated analysis of algal pigments by HPLC. *Mar Chem* **102**(3–4): 267–275. DOI: https://doi.org/10.1016/j.marchem.2006.05.003

Wiencke, C and **Hop, H.** 2016. Ecosystem Kongsfjorden: new views after more than a decade of research. *Polar Biol* **39**(10): 1679–1688. DOI: https://doi.org/10.1007/s00300-016-2032-9

Willis, K, Cottier, FR and **Kwaśniewski, S.** 2008. Impact of warm water advection on the winter zooplankton community in an Arctic fjord. *Polar Biol* **31**: 475. DOI: https://doi.org/10.1007/s00300-007-0373-0

How to cite this article: van de Poll, WH, Kulk, G, Rozema, PD, Brussaard, CPD, Visser, RJW and Buma, AGJ. 2018. Contrasting glacial meltwater effects on post-bloom phytoplankton on temporal and spatial scales in Kongsfjorden, Spitsbergen. *Elem Sci Anth,* 6: 50. DOI: https://doi.org/10.1525/elementa.307

Domain Editor-in-Chief: Jody W. Deming, Ph.D., Department of Biological Oceanography, University of Washington, US

Associate Editor: Jean-Éric Tremblay, Department of Biology, Université Laval, CA

Knowledge Domain: Ocean Science

Submitted: 27 July 2017 **Accepted:** 21 June 2018 **Published:** 10 July 2018

ELEMENTA Science of the Anthropocene

Elem Sci Anth is a peer-reviewed open access journal published by University of California Press.

OPEN ACCESS